



A preprocessing framework for automatic underwater images denoising

Andreas Arnold-Bos, Jean-Philippe Malkasse, Gilles Kervern

► To cite this version:

Andreas Arnold-Bos, Jean-Philippe Malkasse, Gilles Kervern. A preprocessing framework for automatic underwater images denoising. European Conference on Propagation and Systems, Mar 2005, Brest, France. hal-00494314

HAL Id: hal-00494314

<https://hal.science/hal-00494314>

Submitted on 22 Jun 2010

HAL is a multi-disciplinary open access archive for the deposit and dissemination of scientific research documents, whether they are published or not. The documents may come from teaching and research institutions in France or abroad, or from public or private research centers.

L'archive ouverte pluridisciplinaire **HAL**, est destinée au dépôt et à la diffusion de documents scientifiques de niveau recherche, publiés ou non, émanant des établissements d'enseignement et de recherche français ou étrangers, des laboratoires publics ou privés.

A PREPROCESSING FRAMEWORK FOR AUTOMATIC UNDERWATER IMAGES DENOISING

Andreas Arnold-Bos⁽¹⁾, Jean-Philippe Malkasse⁽²⁾, Gilles Kervern⁽²⁾

⁽¹⁾Laboratoire E³I², ENSIETA
2 rue François Verny, 29806 Brest cedex 9, France
Email: arnoldan@ensieta.fr

⁽²⁾Thales Underwater Systems
Route de S^{te} Anne du Portzic, 29238 Brest cedex 3, France
Email: firstname.lastname@fr.thalesgroup.com

SHORT ABSTRACT

A major obstacle to underwater operations using cameras comes from the light absorption and scattering by the marine environment, which limits the visibility distance up to a few meters in coastal waters. Current preprocessing methods typically only concentrate on local contrast equalization in order to deal with the nonuniform lighting caused by the back scattering. We review these techniques, then go further and show that the additional use of adaptive smoothing helps to address the remaining sources of noise and can significantly improve edge detection in the images. Many results on real data are provided and discussed using a custom numerical criterion.

Keywords: underwater vision, denoising, contrast equalization, adaptive smoothing.

1 INTRODUCTION

In the recent few years, the increasing interest in remotely operated vehicles and autonomous underwater vehicles for submarine operations has called for the development of reliable sensors to ensure mission success. Optical cameras seem to be a good choice, as they have a good resolution and are readily available on the market. However, the main drawback to the use of cameras comes from the relatively limited visibility that can be attained: about twenty meters in clear water and less than a few meters in turbid, coastal waters such as in harbors [4].

The propagation process can be divided into three additive components. The exponential decay of the light intensity with distance, called attenuation, leads to a hazy image background. Visibility may indeed be augmented with artificial lighting. Unfortunately, a significant fraction of the power will be reflected by the water towards the camera before actually reaching the objects. This process, known as backscattering, causes undesirable differences of contrast in the image, which mask the details of the scene. Finally, forward scattering, *i.e.* randomly deviated light on its way to the camera, causes blurring of the image features. Macroscopic floating particles (marine snow), can also be considered as unwanted signal. In orders of magnitude, backscattering and marine snow are the greatest degradation factors, forward scattering comes second and attenuation follows closely.

Deconvolution is theoretically possible as the received image can be expressed as the convolution of an ideal image with the modulation transfer function of the water [6]. However many model parameters are needed. First of all, the attenuation and diffusion coefficients that characterize the water turbidity are only scarcely known in tables and can be extremely variable. Next, the most crucial parameter to recover is the depth of a given object point in the scene, which is necessary to correctly estimate the distance traveled by the light. Therefore, to the best of our knowledge, deconvolution has only been used in rather controlled environments so far. Liu *et al.* [5] expose the full deconvolution procedure on the image of a flat object taken in a water tank, which allows for the estimation of the depth. Trucco and Olmos [12] tackle the problem in real-life conditions but assume a top-down point of view, with small variations of the bottom depth; moreover, they use a simplified model where only forward scattering is present. They estimate the medium parameters by using an iterative method on a dedicated quality criterion.

When no specific assumption can be made on the point of view or the turbidity parameters, as in our case, generic image enhancement methods are often employed in the underwater robotics literature. These methods make total abstraction of the image formation process and are usually very simple and fast. They are typically used to correct the contrast disparities caused by the attenuation and backscattering, but the remaining noise level remains high, thus impairing edge detection. In this paper, we explore the use of adaptive smoothing techniques in order to improve the edge detection. Furthermore, we present a simple criterion which allows for a comparison of the enhancement methods and the edge detection robustness.

2 ALGORITHM DESCRIPTION

2.1 Contrast equalization

Many well-known techniques are known to help correcting the lighting disparities in underwater images. As the contrast is non uniform, a global color histogram equalization of the image will not suffice and local methods must be considered. Among all the methods they reviewed, Garcia, Nicosevici and Cufi [2] constated the empirical best results of the illumination-reflectance model on underwater images: if $I(i, j)$ is the original image, and $I_{LP}(i, j)$ its low-pass version, a scaled, contrast-equalized version of I is $I_{eq}(i, j) = I / I_{LP}(i, j)$. The low-pass version of the image is typically computed with a Gaussian filter having a large standard deviation.

After the scaling, pixel values of I_{eq} will present a distribution centered around one, with a small dispersion (especially for poorly contrasted images) except for a few outliers. Therefore, contrast equalization is followed by histogram clipping to reject these outliers:

$$I_{clip}(i, j) = \begin{cases} i_1 & \text{if } I_{eq}(i, j) < i_1, \\ i_2 & \text{if } I_{eq}(i, j) > i_2, \\ I_{eq}(i, j) & \text{else.} \end{cases} \quad (1)$$

where $[i_1..i_2]$ is the 90% percentile interval of the intensity distribution of I_{eq} . Then the dynamic of the image may be expanded so that all available intensity levels $[0..i_{max}]$ are occupied:

$$I_{exp}(i, j) = \frac{I_{clip}(i, j) - i_1}{i_2 - i_1} \cdot i_{max} \quad (2)$$

This method is theoretically relevant because backscattering, which is responsible for most of the contrast disparities, is indeed a slowly varying spatial function. Backscattering is the predominant noise, hence it is sensible for it to be the first noise addressed in the algorithm. However, contrast equalization also corrects the effect of the exponential light attenuation with distance.

2.2 Noises present in the images after equalization

The contrast equalization will generally raise the noise level in poorly contrasted areas of the original image. Indeed, the local gain of the contrast equalization process is:

$$G(i, j) = \frac{1}{I_{LP}(i, j)} \cdot \frac{i_{\max}}{i_2 - i_1} \quad (3)$$

The standard deviation of the noise at location (i, j) will also be multiplied by $G(i, j)$; consequently, the lower the intensity, the higher the noise level. Gain G affects all types of noises remaining in the image, as the additive Gaussian noise of the camera electronics, the quantification noise, which can all be considered as Gaussian white noise. However, these noises are often small in front of the noise produced by the water, of which we shall now give a brief summary.

Apart from forward scattering, which has a blurring effect, macroscopic floating particles producing images of the size of a pixel can be present as well: it may be, for instance, sand raised by the motion of a diver, or small plankton particles. These particles are, *per se*, part of the scene, but cause generally unwanted signal. We see them as an additive noise, of distribution clearly not Gaussian yet still reasonably similar, because the particles will act as (secondary) sources of attenuated and diffused light. It is important to stress the local nature of this noise, and the problems it causes in edge detection, because it is likely to cause falsely detected edges.

2.3 Use of adaptive smoothing to increase edge detection robustness

Edge detectors such as the Canny-Deriche algorithm [1] use a linear filter of typical width α akin to the Gaussian filter to smooth the image in the orthogonal direction to the computed derivative. This helps to reduce noise and increases the edge detectability. In the underwater context, noise is generally important so large α values are needed; doing so results in badly localized and less precise object shapes. Indeed, the linear smoothing filter does not adapt itself to the local noise intensity or the presence of edges, so the filtering level is overevaluated on some parts of the image. This was our motivation for adding an adaptive image smoothing stage between the contrast equalization and the edge detection. The principle behind adaptive smoothing is that the image is filtered less where edges are present, hence preserving their good visibility. We have experimented anisotropic filtering and complex wavelets as possible means to reduce the influence of the aforementioned noises. Before providing the results, we shall briefly describe how these methods are used.

2.4 Anisotropic filtering

Anisotropic filtering was introduced in a seminal article by Perona and Malik [8]. Basically, it consists in solving iteratively a modified version of the heat diffusion equation on the image, using a control function c of the gradient:

$$\begin{cases} \frac{\partial i}{\partial t} = \lambda \cdot \text{div} \left(c(|\overrightarrow{\text{grad}} i|^2) \overrightarrow{\text{grad}} i \right) \\ i(t = 0, x, y) = i_0(x, y) \end{cases} \quad (4)$$

Smoothing increases with time t and the diffusion coefficient λ . In order to account for the local noise amplification caused by the contrast equalization, we write:

$$\lambda(i, j) = \lambda_0 \cdot G(i, j) \quad (5)$$

Control function c tends to one to allow diffusion when the gradient is small (*i.e.* in uniform areas of the image). When the gradient gets large (in the vicinity of edges), c tends towards zero.

Various forms have been proposed for c . We use the function proposed by Sochen, Kimmel and Mallardi [10], because it optimizes the tradeoff between a small diffusion in the direction of the gradient, and a large tangential diffusion:

$$c(|\overrightarrow{\text{grad}} i|) = \frac{1}{\sqrt{1 + |\overrightarrow{\text{grad}} i|^2}} \quad (6)$$

2.5 Wavelet filtering

Time-frequency methods have also been widely used to denoise images, especially bi-orthogonal or “symlet” wavelet decomposition. Known problems of these methods are the following:

1. they are not translation independent and thus may corrupt the phase of the signal, which distorts edges;
2. an automatic thresholding method of the wavelets coefficients is not always available.

We followed Kovesi [3] who proposed to use complex-valued log-Gabor wavelets so as to have an approximation of the amplitude and the phase of the signal at various scales. Then, only the amplitude of the coefficients is shrunk by the estimated noise contribution at that scale, so as to preserve the phase of the signal. Noise is assumed to be Gaussian and white, so the distribution of the amplitude of the wavelets coefficients at each scale follows approximately a Rayleigh distribution. Of the ideal image, only edges (about 5 % of the pixels) contribute at the smallest scale and the majority of the coefficients correspond to noise; their mean and variance can therefore be easily computed. Then, because the noise is supposed to be white, its contribution at a given scale is proportional to the bandwidth of the wavelet corresponding to that scale. However, unlike Kovesi’s original algorithm, we do not use a constant threshold over space, but instead correct it by factor $G(i, j)$ so that heavier filtering is done where the initial image was dark. Note that the assumption of a Gaussian white noise is false in our case, but the noise distribution observed in uniform zones of our images were close enough. The principal advantage of Kovesi’s method is that no constants tuning is necessary after initial setting. Note that other wavelet-based denoising schemes exist that behave well on edges, such as the curvelets [11], which may be investigated in the future in our context.

3 EXPERIMENTS

3.1 Qualitative results

We performed our experiments on miscellaneous images with unknown turbidity characteristics. These images present typical noise levels for underwater conditions. **Fig. 1** offers a visual comparison of the effect of the two stages of our preprocessing on the original image. Contrast equalization enhances visibility, yet it may create halos around strongly contrasted objects of size similar to the Gaussian kernel (visible on image c, around fishes). We found that a good tradeoff between equalization and small halos could be found by allowing the standard deviation of the kernel to be five to ten percent of the image diagonal length. Noise remaining after contrast equalization is visibly reduced after adaptive smoothing. Kovesi’s method was used to perform the smoothing, but anisotropic diffusion gives slightly better solutions, with sharper edges, as seen in **fig. 2**. However, anisotropic filtering has two drawbacks: a lengthy computation time and the fact that diffusion constants must be manually tuned. Kovesi’s method is faster and automatic. **Fig. 3** displays the edges as found by the Canny-Deriche detector for the

four previous images. In all cases, the thresholds and smoothing parameters of the Canny detector are the same. More edges are detected after contrast equalization, but they include false positives. Smoothing helps to cut down on edges corresponding to noise.

3.2 Quantitative results

Contrast is often suggested as a means to assess the gain in underwater image preprocessing algorithms. Various contrast criteria have been proposed in the literature [7]. Global contrast criteria, the simplest of which is the variance of the image, is not usable because of the nonuniform lighting in raw images. Local criteria are generally very complicated and not very condensed, thus heavier to use.

To assess the quality of enhancement methods, we propose a new, synthetic criterion. We base it on a very general result by Pratt [9]: for most well-contrasted and noise-free images, the distribution of the gradient magnitude histogram is closely exponential, except for a small peak at low gradients corresponding to homogeneous zones. When images have such a gradient distribution, edges are generally easily discernible from noise by a simple thresholding of the gradient. On the contrary, for an image heavily corrupted by noise, or badly contrasted, the gradient magnitude distribution will be very different. For instance, if we consider the extreme case of an image consisting in pure Gaussian white noise, the two components of the gradient will be normally distributed (as differences of normally distributed random variables); and the magnitude of the gradient will follow a Rayleigh distribution. On the other hand, a badly contrasted image will have more low gradients than usual, so the distribution will not be exponential.

We note i the gradient magnitude and $h(i)$ the gradient magnitude histogram (computed on typically $N = 128$ bins and normalized by its sum), then we perform a linear regression on $\ln h(i)$, as shown in **fig. 4**:

$$\ln \bar{h}(i) = a - b.i \quad (7)$$

In practice, not all the gradient magnitude range is used for the regression, because noise appears in $\ln h(i)$ at high gradients. This noise results from sampling effects for low histogram counts.

In our experiments, the magnitude range went from $i = 1$ to $N' = 2/3N$.

Our robustness criterion is linked to the variance of the linear regression, which measures the closeness of the histogram with an exponential distribution. The closer the robustness is to one, the better the enhancement:

$$R = \exp \left(-\frac{1}{N' - 1} \sum_{i=1}^{i=N'} (\ln h(i) - \ln \bar{h}(i))^2 \right) \quad (8)$$

Robustness is indicated in **fig. 3** for the images presented in this paper. The values taken by the criterion confirm our intuition concerning the image quality. R takes lower values for images where the sea bottom is not visible or made of sand, as the uniform background perturbs the gradient statistics; but generally speaking the robustness criterion is higher for smoothed images than for just contrast-equalized images, which in turn have a higher robustness than raw images.

4 CONCLUSION

In this paper, we showed that the standard method consisting in simply equalizing the contrast of the images is not sufficient enough in many cases to allow for a robust edge detection. To correct this, we benchmarked two classes of adaptive smoothing methods: anisotropic filtering and Kovess's phase preserving wavelet filtering. This helps to address the remaining noise

sources in the image (the captor and the macroscopic floating particles). We showed that the two methods give arguably similar visual results and both improve edge detection. However Kovési's approach provides a self-thresholding mechanism, which allows for a fully automatic denoising. We also proposed a simple, condensed numerical criterion to assess the quality of the restoration procedure, which generally agrees with intuition.

ACKNOWLEDGMENTS

The first author wishes to thank Thales Underwater Systems for having welcomed him as a student intern during his *Diplôme d'Etudes Approfondies* in Signal and Image processing (Supaero, Toulouse) final project.

REFERENCES

- [1] R. Deriche. Using Canny's criteria to derive a recursively implemented optimal edge detector. *The International Journal Of Computer Vision*, 1(2):167–187, May 1987.
- [2] R. Garcia, T. Nicosevici, and X. Cufi. On the way to solve lighting problems in underwater imaging. In *Proceedings of the IEEE Oceans 2002*, pages 1018–1024, Oct. 2002.
- [3] P. Kovési. Phase preserving denoising of images. In *Proceedings of The Australian Pattern Recognition Society Conference DICTA'99*, Dec. 1999.
- [4] M. Legris, K. Lebart, F. Fohanno, and B. Zerr. Les capteurs d'imagerie en robotique sous-marine: tendances actuelles et futures. *Traitement du Signal*, 20:137–164, 2003.
- [5] Z. Liu, Y. Yu, K. Zhang, and H. Huang. Underwater image transmission and blurred image restoration. *SPIE Journal of Optical Engineering*, 40(6):1125–1131, June 2001.
- [6] B. L. McGlamery. A computer model for underwater camera systems. *SPIE Ocean Optics VI*, 28, 1979.
- [7] E. Peli. Contrast in complex images. *Journal of the Optical Society of America*, 7(10):2032–2040, Oct. 1990.
- [8] P. Perona and J. Malik. Scale-space and edge detection using anisotropic diffusion. *IEEE Transactions on Pattern Analysis and Machine Intelligence*, 12(7):629–639, July 1990.
- [9] W. K. Pratt. *Digital Image Processing*. John Wiley & Sons, New York, 1991.
- [10] N. Sochen, R. Kimmel, and R. Mallardi. A geometrical framework for low-level vision. *IEEE Transactions on Image Processing, Special Issue on PDE-based Image Processing*, 7(3):310–318, 1998.
- [11] J.-L. Starck, E. J. Candès, and D. L. Donoho. The curvelet transform for image denoising. *IEEE Transactions on Image Processing*, 11(2):670–684, June 2002.
- [12] E. Trucco and A. O. Antillon. Self-tuning underwater image restoration. In press.

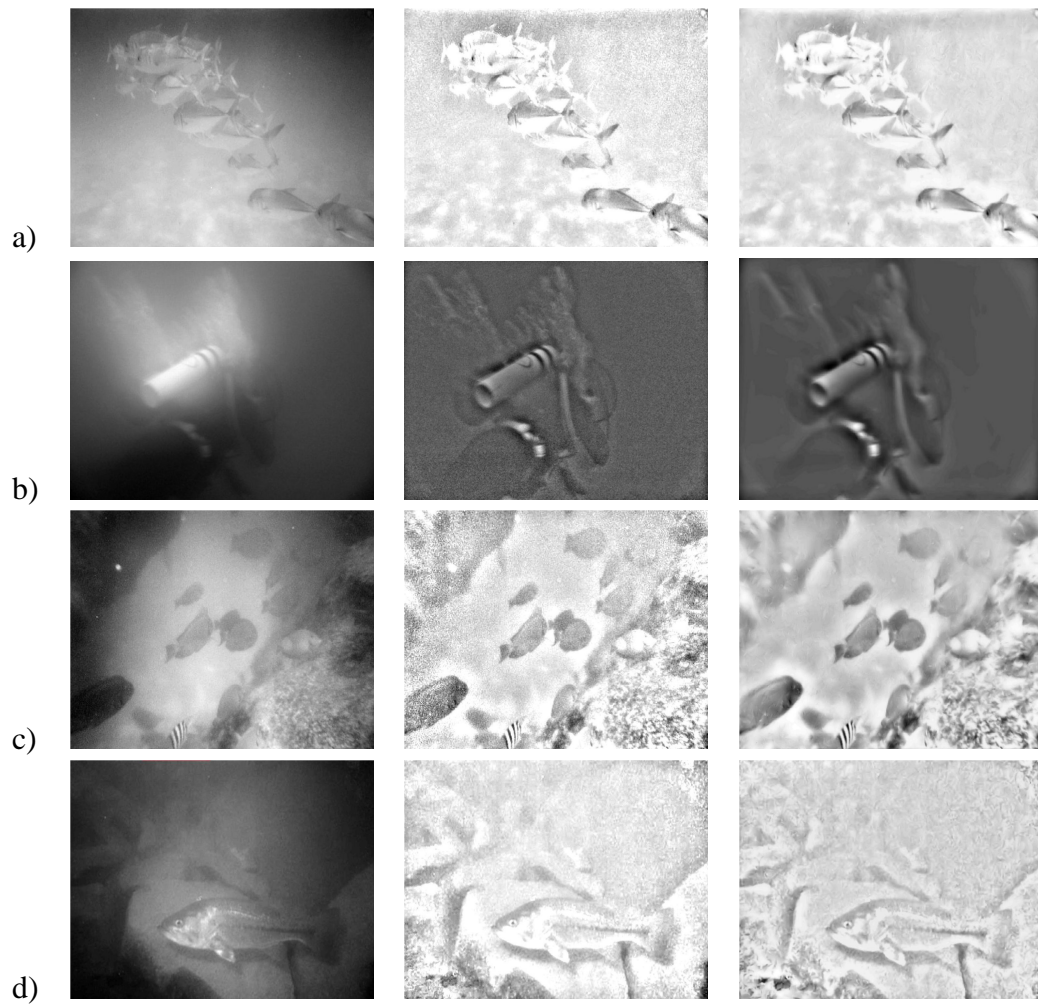


Fig. 1: *Benefits of adaptive smoothing. Left: original image. Middle: after contrast normalization and histogram clipping. Right: after Kovesi wavelet filtering.*

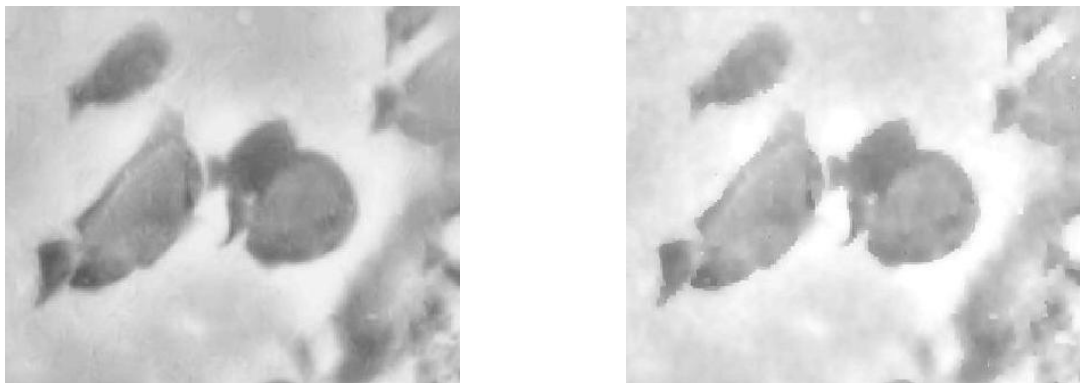


Fig. 2: *Close-up view of image c) for comparison between Kovesi's wavelet filtering (left) and anisotropic filtering (right).*

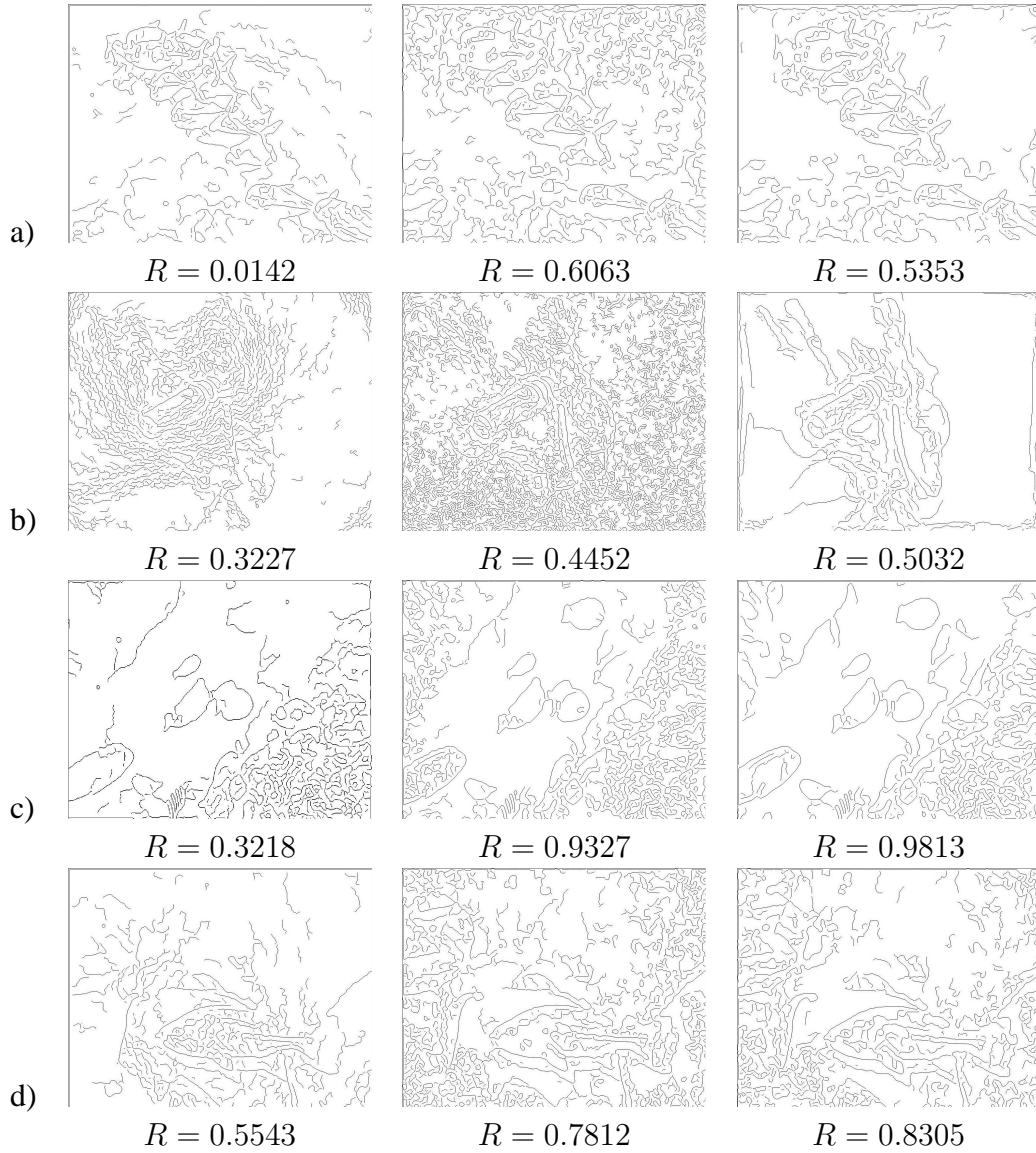


Fig. 3: Comparison of edge detectability robustness. More edges are detected after contrast equalization; and fewer false positives are found after adaptive smoothing.

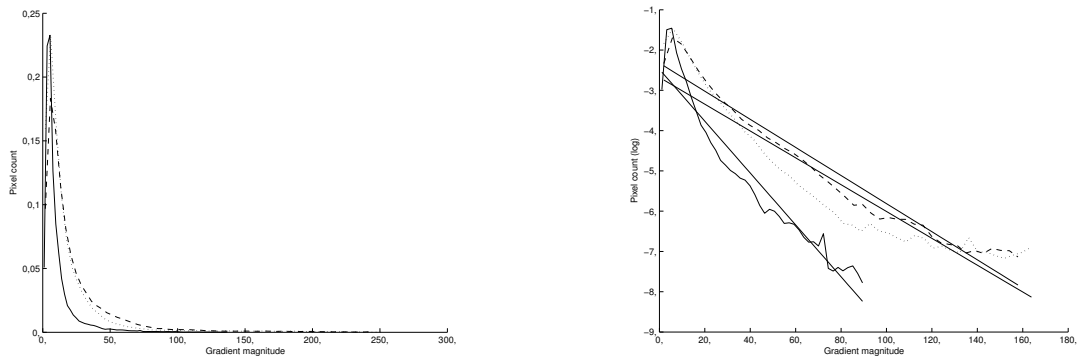


Fig. 4: Gradient magnitude histogram for image d). Plain line: original image, dotted line: after equalization, dashed line: after smoothing. Gradient was computed with the Canny-Deriche filter, $\alpha = 0.5$.